

Source apportionment of fine particles and its chemical components over the Yangtze River Delta, China during a heavy haze pollution episode



L. Li ^{a, b, *}, J.Y. An ^{a, b}, M. Zhou ^{a, b}, R.S. Yan ^{a, b}, C. Huang ^{a, b}, Q. Lu ^{a, b}, L. Lin ^{a, b}, Y.J. Wang ^c, S.K. Tao ^{a, b}, L.P. Qiao ^{a, b}, S.H. Zhu ^{a, b}, C.H. Chen ^{a, b}

^a State Environmental Protection Key Laboratory of the Cause and Prevention of Urban Air Pollution Complex, Shanghai 200233, China

^b Shanghai Academy of Environmental Sciences, Shanghai 200233, China

^c School of Environmental and Chemical Engineering, Shanghai University, Shanghai 200444, China

HIGHLIGHTS

- A high PM_{2.5} episode over the YRD was simulated using the CMAQ modeling system.
- Particulate matter source apportionment technology was applied to study the sources contributing to PM_{2.5}.
- Regional and source category contributions to PM_{2.5} in the YRD were analyzed.

ARTICLE INFO

Article history:

Received 27 February 2015

Received in revised form

13 June 2015

Accepted 29 June 2015

Available online 6 July 2015

Keywords:

Fine particulate matter

Particulate matter source apportionment technology

Yangtze River Delta

CAMx

ABSTRACT

An extremely high PM_{2.5} pollution episode occurred over the eastern China in January 2013. In this paper, the particulate matter source apportionment technology (PSAT) method coupled within the Comprehensive air quality model with extensions (CAMx) is applied to study the source contributions to PM_{2.5} and its major components at six receptors (Urban Shanghai, Chongming, Dianshan Lake, Urban Suzhou, Hangzhou and Zhoushan) in the Yangtze River Delta (YRD) region. Contributions from 4 source areas (including Shanghai, South Jiangsu, North Zhejiang and Super-region) and 9 emission sectors (including power plants, industrial boilers and kilns, industrial processing, mobile source, residential, volatile emissions, dust, agriculture and biogenic emissions) to PM_{2.5} and its major components (sulfate, nitrate, ammonia, organic carbon and elemental carbon) at the six receptors in the YRD region are quantified. Results show that accumulation of local pollution was the largest contributor during this air pollution episode in urban Shanghai (55%) and Suzhou (46%), followed by long-range transport (37% contribution to Shanghai and 44% to Suzhou). Super-regional emissions play an important role in PM_{2.5} formation at Hangzhou (48%) and Zhoushan site (68%). Among the emission sectors contributing to the high pollution episode, the major source categories include industrial processing (with contributions ranging between 12.7 and 38.7% at different receptors), combustion source (21.7–37.3%), mobile source (7.5–17.7%) and fugitive dust (8.4–27.3%). Agricultural contribution is also very significant at Zhoushan site (24.5%). In terms of the PM_{2.5} major components, it is found that industrial boilers and kilns are the major source contributor to sulfate and nitrate. Volatile emission source and agriculture are the major contributors to ammonia; transport is the largest contributor to elemental carbon. Industrial processing, volatile emissions and mobile source are the most significant contributors to organic carbon. Results show that the Yangtze River Delta region should focus on the joint pollution control of industrial processing, combustion emissions, mobile source emissions, and fugitive dust. Regional transport of air pollution among the cities are prominent, and the implementation of regional joint prevention and control of air pollution will help to alleviate fine particulate matter concentrations under heavy pollution case significantly.

© 2015 Elsevier Ltd. All rights reserved.

* Corresponding author. State Environmental Protection Key Laboratory of the Cause and Prevention of Urban Air Pollution Complex, Shanghai 200233, China.

E-mail address: lili@saes.sh.cn (L. Li).

1. Introduction

With the fast development of urbanization, industrialization and motorization, the energy consumption and anthropogenic emissions increase quickly in eastern China. Heavy haze pollution episodes occur frequently (Du et al., 2011; Huang et al., 2012; Kang et al., 2013), which has attracted much interest and more attention of researchers in recent years (Wang et al., 2009). A heavy haze episode occurred in eastern China in January, 2013, which lasted for quite a long time period, and its pollution level was very high, attracting the attention of all society (Zhou et al., 2013; Wang et al., 2013). The hourly maximum concentration of PM_{2.5} in Beijing reached 680 µg/m³, while the hourly PM_{2.5} in Shanghai, Nanjing and Hangzhou exceeded 250 µg/m³ during the episode. High PM_{2.5} will cause visibility deterioration (Tie et al., 2009; Zhang et al., 2010), affect the global climate (Zhang, 2007) and seriously harm human health (Craig et al., 2008; Huang et al., 2009; WHO, 2009). However, studies on the source apportionment of PM_{2.5} and its chemical components in the Yangtze River Delta (YRD) during heavy pollution episode are still quite limited. Therefore, it is of great significance to diagnose the source and region contribution to high PM_{2.5} concentrations, which will provide scientific and technological support for the prevention and control of heavy haze in the YRD region.

Many researches have performed PM_{2.5} source apportionment at many locations throughout the world. In previous studies, chemical mass balance (CMB) and positive matrix factorization (PMF) methods are the most commonly used receptor models in particulate matter source apportionment using observed air quality data. The CMB model has been widely used in cities such as Los Angeles (Schauer et al., 1996), San Joaquin Valley (Schauer and Cass, 2000), southeastern America (Zheng et al., 2002), Pittsburgh (Subramanian et al., 2006), Beijing (Wang et al., 2009), Tianjin (Dai et al., 1995), Hangzhou (Bao et al., 2010) and Nanjing (Huang et al., 2006), etc. The PMF method has also been applied in Seoul (Heo et al., 2009) and St. Louis (Song et al., 2008). Particulate matter source apportionment can also be obtained from source-oriented numerical air quality models using methods based on sensitivity analysis, including Brute Force Method (BFM) (Zhang et al., 2005; Koo et al., 2009) and Decoupled Direct Method (DDM) (Dunker, 1981). The numerical simulation study on PM_{2.5} has been done by many experts in the Yangtze River Delta region (Li et al., 2008, 2011; Wang et al., 2013), Beijing and its surrounding area (Wang et al., 2014) and the Pearl River Delta region (Chen et al., 2009). These results have provided meaningful achievements for diagnosing PM_{2.5} pollution sources both locally and regionally. However, the analytical method based on receptor models can analyze the particulate matter sources and their relative contributions both qualitatively and quantitatively, however, it can't accurately locate the sources, and is unable to determine the sources of secondary pollutants as well (Richards et al., 1999). The study on precursors' effects on air pollution based on brute force method (BF) is more intuitive and easy to use, but it is not computationally efficient due to the requirements of individual simulation for each scenario. The DDM method is computationally efficient for emission change scenarios (Dunker et al., 2002) compared to BF, but it cannot quantify the exact contribution from different regions and emission sectors within one-run.

In this study, the three-dimensional air quality numerical model, Comprehensive Air Quality Model with extensions (CAMx), coupled with Particulate Matter Source Apportionment Technology (PSAT), is applied to analyze the region and source category contribution to PM_{2.5} and its chemical components in four major cities of the YRD region. It can quantitatively diagnose pollution source area and emission source categories contributing to PM_{2.5}

(Ying and Kleeman, 2006; Wagstrom et al., 2008). Contributions from 4 source areas (including Shanghai, South Jiangsu, North Zhejiang and Super-region) and 8 source sectors (including combustion, industrial processing, mobile source, residential, dust, volatile emissions, agriculture and biogenic source) to PM_{2.5} and its major components (sulfate, nitrate, ammonia, organic carbon and elemental carbon) at the 6 receptors (urban Shanghai, Chongming, Dianshan Lake, Urban Suzhou, Hangzhou and Zhoushan) in the Yangtze River Delta (YRD) region are quantified. This study aims at providing scientific basis for the joint regional heavy air pollution control.

2. Methodology

2.1. Model description

CAMx is an advanced photochemical diffusion model based on the framework of 'one atmosphere', which comprehensively simulates and evaluates gaseous and particulate matters in cities and regions (ENVIRON, 2011). PSAT is an important extension function of CAMx, which can be applied in pollution diagnosis of source categories and geographic regions of PM_{2.5} and its major chemical components (Wagstrom et al., 2008). In the PSAT method, reactive tracers are added to various pollution sources to apportion primary particulate matter, secondary aerosol and gaseous precursors of secondary organic aerosol (SOA). The chemical components in fine particles that PSAT traced mainly include sulfate, nitrate, ammonium, mercury, primary and secondary organic aerosols, elemental carbon, crust particles and others. One basic assumption of PSAT is tracing main precursor contributions to each PM, for example, tracing sulfur oxide of sulfate, tracing nitrogen oxides of nitrate, tracing ammonia of ammonium salt. Detailed information about PSAT has been described in the CAMx user's manual (<http://www.camx.com>).

2.2. Model setup

The model domain is based on a Lambert Conformal map projection, using a one-way nested mode with grid resolutions of 81 km, 27 km, 9 km and 3 km, as shown in Fig. 1. The chemical mechanism, Carbon Bond 05 (Yarwood et al., 2005) as gas-phase chemistry, RADM as aqueous-phase chemistry, ISORROPIA (Nenes et al., 1998) as inorganic aerosol and SOAP for secondary organic aerosol formation and partitioning are selected in CAMx. The meteorological data is from the results of the Fifth-Generation NCAR/Penn State Mesoscale Model (MM5), its driving and the initial fields are selected from the global reanalysis data of NCEP. The mother domains for both MM5 and CAMx are centered at (110°E, 34°N). The pollution episode chosen is 1–31 January 2013, when a heavy pollution episode occurs in eastern China. The initial conditions of CAMx are prepared by running the model five days ahead of the start date. The boundary condition (BC) for the nested domains are extracted from the CAMx concentration files of the larger domain. The CAMx model employs 14 vertical layers of varying thickness with denser layers in the lower atmosphere to better resolve the mixing height.

The anthropogenic emission inventory used for D04 domain is the updated atmospheric pollutant emission inventory of the Yangtze River Delta region which was established based on a bottom-up method by our research group (Huang et al., 2011; Li et al., 2011), while D01–D03 emission inventory is the INTEX-B emission inventory established by Zhang et al. (2009).

Four source regions are established, including Shanghai, south Jiangsu, north Zhejiang and long-range transport outside the D04 region, as shown in Fig. 1 (right). Eight emission sectors are

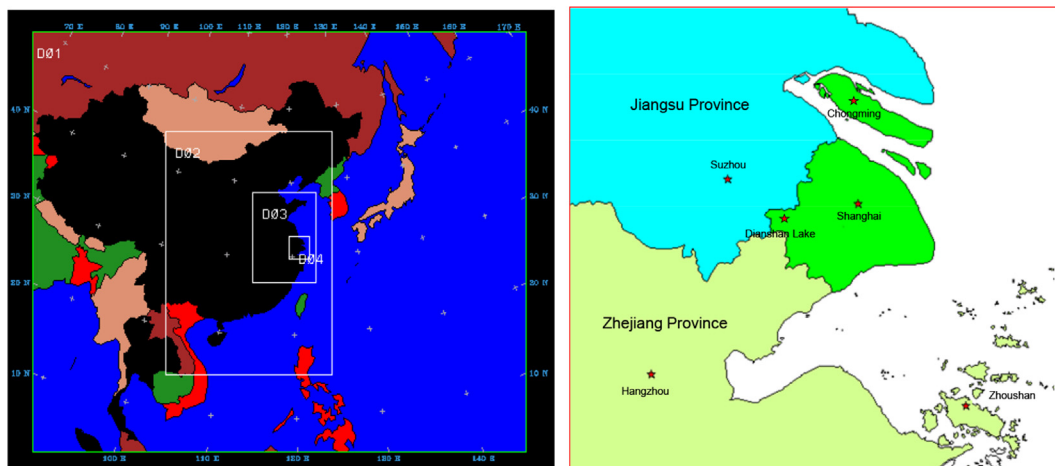


Fig. 1. One-way nested model domain (left) and the inner YRD model domain (right).

separated in the regional emission inventory, including combustion source, industrial processing, mobile source, dust, agricultural, volatile, residential and biogenic source. Each emission source is described in Table 1. Six receptors are selected to do the $PM_{2.5}$ source apportionment, including Urban Shanghai (SAES), Chongming (CM), Dianshan Lake (DSL), Suzhou (SZ), Hangzhou (HZ) and Zhoushan (ZS), locations of the six receptors are shown in Fig. 1 (right). Among the six receptors, there are two urban sites including Shanghai and Suzhou. Chongming is a typical site located in the transport path between Shanghai and Jiangsu. Dishan Lake is situated among the joint area of Jiangsu, Shanghai and Zhejiang, and with rare local emissions nearby. Zhoushan is located quite close to the eastern sea, and there is small local anthropogenic emissions.

3. Model performance

Hourly concentrations of $PM_{2.5}$ measured during the period 6–31 January 2013 at 8 observational sites (including SAES, Luwan, JingAn, Putuo, Pudong, Dianshanhu, Yangpu) located in Shanghai are used to evaluate the model performance.

The simulation of $PM_{2.5}$ chemical compositions are evaluated against observations made at the supersite in Shanghai Academy of Environmental Sciences (SAES). The measurements are collected simultaneously at the surface site of SAES. The hourly $PM_{2.5}$ concentrations are measured by Thermo Fisher commercial instruments β -ray particulate monitor. The water soluble ions are measured by MARGA ADI 2080 online analyzer for monitoring of aerosols, and the organic carbon and elemental carbon are measured by the carbon analyzer provided by Sunset laboratory Inc. Statistical methods of model performance include the normalized mean bias (NMB), normalized mean error (NME), mean

fractional bias (MFB), mean fractional error (MFE) and index of agreement (I) (USEPA, 2007). Fig. 2 shows the comparisons between predicted and observed hourly $PM_{2.5}$ concentrations at eight sites in Shanghai. Besides, Fig. 3 gives the time series of the hourly $PM_{2.5}$ chemical components at the SAES supersite, including sulfate, nitrate, ammonia, elemental carbon and organic carbon. Table 2 shows the statistical results between predicted and observed $PM_{2.5}$ and its chemical components at the SAES supersite, while Table 3 shows the statistical evaluation of model performance on $PM_{2.5}$ at different sites.

Model evaluation shows that NMB and NME simulation of $PM_{2.5}$ is 11% and 49%, respectively. Simulated concentration of $PM_{2.5}$ components is relatively lower than the observed data, while NMB values are all negative. Among the three major water soluble ions, the predicted $SO_4^{2-}_{2.5}$ is relatively low, trend of the simulated $NO_3^{-}_{2.5}$ is consistent with actual observed data, with the IOA of 0.64. The predicted $NH_4^{+}_{2.5}$ peak value is obviously lower than the observed data. The trend of elemental carbon is similar to organic carbon. Some researchers found that winter underestimation of sulfate is a common issue detected with CMAQ over Europe (Matthias, 2008), which can be explained by a lack of model calculated oxidants or missing reactions (Kasibhatla et al., 1997). The biases of $EC_{2.5}$ can be attributed to the probable underestimation of primary carbonaceous emission (Monks et al., 2009). Some researches (Volkamer et al., 2006; Basart et al., 2012) have found that SOA is commonly underestimated in most current models due to the state-of-science concerning SOA formation pathways (Appel et al., 2008; Foley et al., 2010). However, $PM_{2.5}$ is overestimated by 11% at the SAES site due to overestimation of the fugitive dust, which is of great uncertainty in the regional emission inventory. There are not so many significant high values during the simulation period of the above two components, while the

Table 1
Split of emission sectors.

NO.	Source Categories	Description
1	Combustion	Coal and oil combustion from industrial boilers, kilns, power plants.
2	Industrial processing	Emissions from steel, coke, cement production, petrochemical and chemical processes, etc.
3	Mobile source	Gasoline engine exhaust, diesel engine exhaust, evaporation emissions, marine and aircraft emissions.
4	Dust	Particulate matter emissions from road, construction, and yard dust.
5	Agricultural	Ammonia emissions from livestock and poultry breeding, fertilizer application, biomass combustion.
6	Volatile	Cooking fume, paintings, oil-gas evaporation, urban ammonia emissions.
7	Residential	Residential combustion emissions.
8	Biogenic	Biogenic emissions.

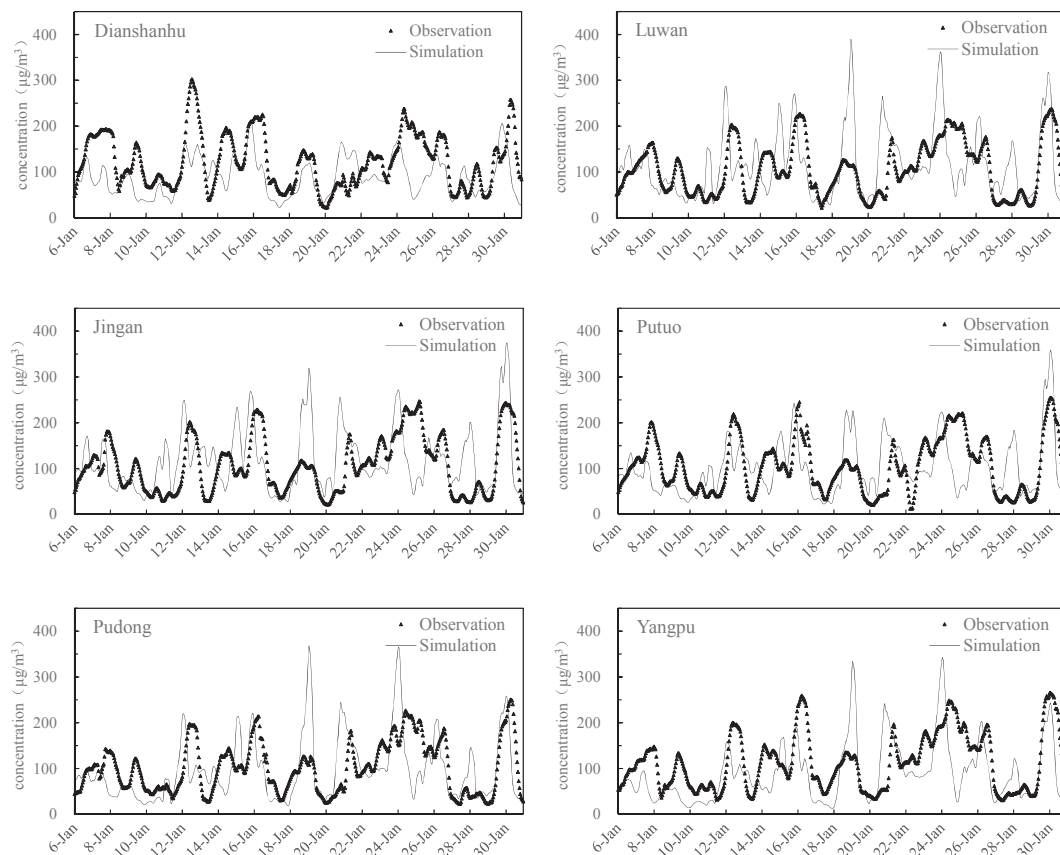


Fig. 2. Time series of the hourly predicted and observed $PM_{2.5}$ concentrations at eight sites in Shanghai.

simulated concentration is much more consistent with the observed value in the low value zone. Overall, the trend of simulated value and observed data of the hourly $PM_{2.5}$ concentration matches well, the simulation result can basically reflect the change of $PM_{2.5}$ concentration in January. Simulation performance is acceptable according to the evaluation standard recommended by U.S. EPA (2007).

4. Results and discussion

4.1. Meteorological conditions

During January, 2013, the surface weather system in eastern China was very stable. The circulation was effected by an extra tropical cyclone and blocking high pressure. The cold air from high latitude area affected most of China through its movement down to the south. The activities of the cold air over the continent were frequent under this influence. The temperature experienced a process of “cold – gradually warm – cold again” in the YRD region. Westerly wind prevails during this period with the average wind speed of less than 1 m/s, which is significantly lower than the annual average wind speed. Shanghai was controlled by ground high pressure (Fig. 4) with weak air flow. Static wind or southwest wind with strong temperature inversion near the ground occurred at night under the control of this stable weather system. Temperature inversion occurred frequently during the pollution episode, which accelerated ground accumulation and pollution accumulative growth rate (Fig. 5). The average relative humidity was 70%, and the maximum relative humidity reached 91.8%, the relative high humidity accelerated the growth of fine particles (Guo et al., 2010).

4.2. $PM_{2.5}$ pollution characteristics

Observed data shows that the average $PM_{2.5}$ concentration during the haze pollution episode in urban Shanghai area in January was $89.5 \mu\text{g}/\text{m}^3$, while it reached $124.08 \mu\text{g}/\text{m}^3$ at Dianshan Lake, indicating a more significant regional air pollution influence than urban Shanghai area. Fig. 6 shows the time series of the hourly averaged meteorological parameters and $PM_{2.5}$ concentrations at urban Shanghai, Chongming and Dianshan Lake. When the wind speed is small and relative humidity is high, the $PM_{2.5}$ concentrations can reach very high at three different sites, showing that regional air pollution is obvious in winter in the YRD region. It is also found that the $PM_{2.5}$ at Dianshan Lake is generally higher than those in Chongming and urban Shanghai, indicating that regional contribution is more significant to $PM_{2.5}$ at the Dianshan Lake site.

4.3. $PM_{2.5}$ source apportionment in major cities of the YRD

4.3.1. Spatial distribution of $PM_{2.5}$ regional contribution

The model predicted regional contribution to $PM_{2.5}$ at the six receptors in the YRD are shown in Fig. 6. As shown in the figure, the high $PM_{2.5}$ concentration was caused by the combined effect of both local pollution accumulation and long-range transport. At the urban Shanghai (SAES) site, the model predicted $PM_{2.5}$ contribution shows that 55% is from local Shanghai area, 37% from super-regional transport and 6% from south Jiangsu region. At the urban Hangzhou (HZ) and Zhoushan (ZS) receptors, the super-regional transport outside the 3 km modeling domain dominates the high $PM_{2.5}$ concentrations (57% at Hangzhou and 68% at Zhoushan). This is mainly because the locations of these two sites are quite close to the modeling domain boundary. The strong wind in winter brings

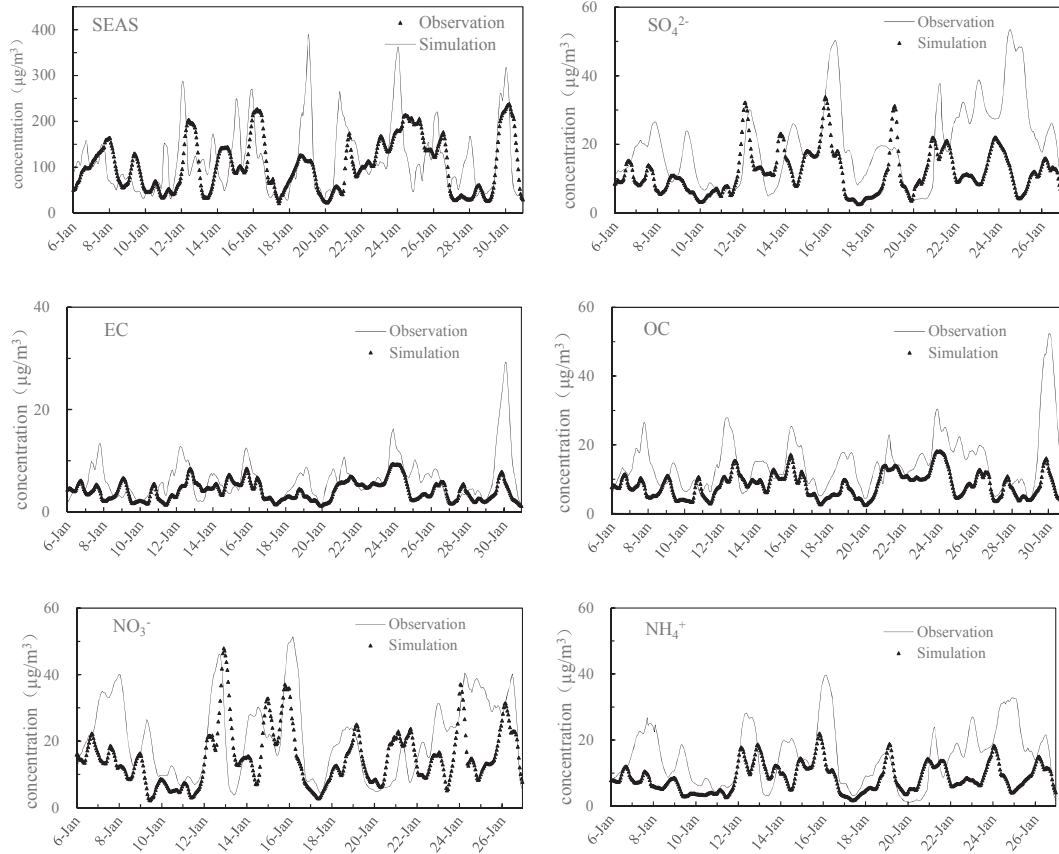


Fig. 3. Time series of the hourly predicted PM_{2.5} chemical components at the SAES supersite.

Table 2
Statistical data of the predicted and observed PM_{2.5} and its chemical components at SAES.

Species	Samples	Data source	Hourly average (µg/m ³)	Hourly maximum (µg/m ³)	Hourly minimum (µg/m ³)	NMB (%)	NME (%)	MFB (%)	MFE (%)	IOA
PM _{2.5}	600	Simulation	101.9	239.4	25.2	11	49	12	49	0.64
		Observation	91.8	210.3	13.6					
SO ₄ ²⁻	504	Simulation	12.0	33.8	2.6	-40	52	-32	47	0.49
		Observation	19.9	53.5	3.9					
NO ₃ ⁻	504	Simulation	15.2	47.9	2.1	-28	45	3	51	0.64
		Observation	21.1	51.4	3.8					
NH ₄ ⁺	504	Simulation	8.7	22.0	1.8	-41	51	10	47	0.55
		Observation	14.8	39.7	1.1					
OC	600	Simulation	8.4	18.1	2.3	-42	45	7	47	0.54
		Observation	14.6	52.3	3.6					
EC	600	Simulation	4.2	9.4	1.2	-32	43	11	52	0.55
		Observation	6.2	29.3	1.3					

Table 3
Statistical data of the predicted and observed PM_{2.5} at different sites.

Species	Samples	Data source	Hourly average (µg/m ³)	Hourly maximum (µg/m ³)	Hourly minimum (µg/m ³)	NMB (%)	NME (%)	MFB (%)	MFE (%)	I
Dianshanhu	600	Simulation	88.7	302.0	21.7	-28	41	-30	47	0.62
		Observation	123.6	213.8	22.0					
Luwan		Simulation	116.5	237.7	21.6	10	51	7	47	0.63
		Observation	105.7	390.0	25.9					
Jingan		Simulation	118.3	246.8	21.3	11	54	11	52	0.61
		Observation	107.0	374.8	27.5					
Putuo		Simulation	102.1	254.6	12.5	-3	48	-1	52	0.66
		Observation	105.3	359.0	21.9					
Pudong		Simulation	98.1	250.3	22.6	-4	48	-9	48	0.65
		Observation	102.4	368.1	18.4					
Yangpu		Simulation	89.9	265.2	30.4	-21	45	-30	54	0.69
		Observation	114.2	342.7	12.4					

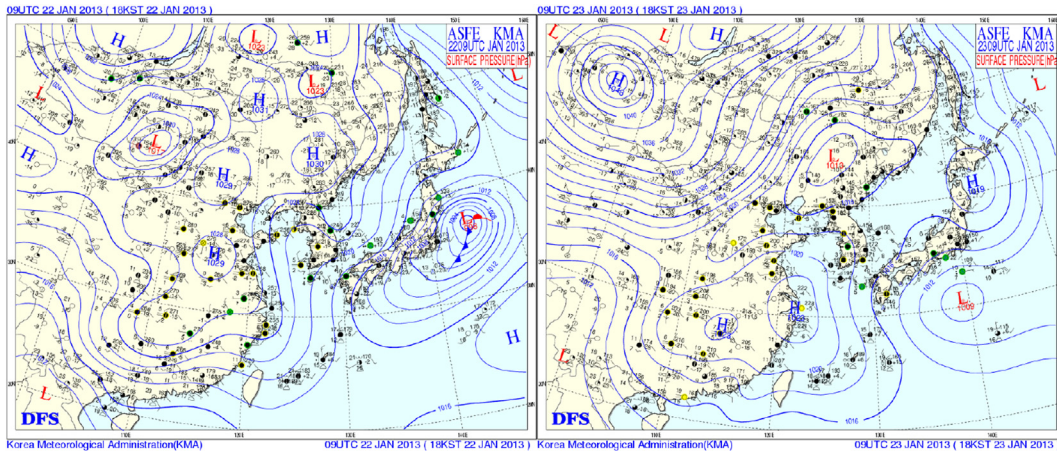


Fig. 4. Weather patterns at the surface level over the eastern Asia at 17:00 during Jan. 22–23, 2013 (from Korea Meteorological Administration).

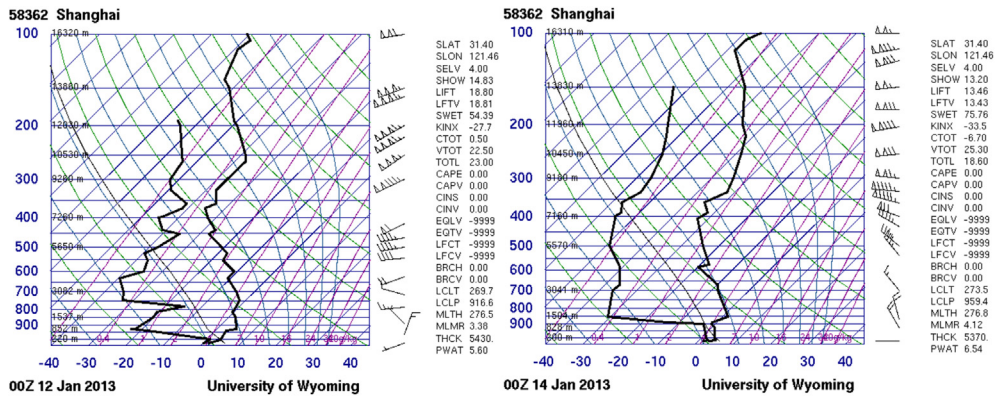


Fig. 5. Vertical temperature profiles in Shanghai at 8:00 am on Jan. 12 and 14, 2013 (<http://weather.uwo.edu/upperair/sounding.html>).

quite a lot of both gas precursors and directly emitted fine particles to the receptor regions. The contribution from super-regional transport to surface PM_{2.5} at the Hangzhou receptor is much higher than the Suzhou site (44%), since it is located at the

southwest corner of the modeling domain, and its upwind regions are mostly outside the modeling domain under the northerly and northwest wind direction in winter time. Dianshan Lake (DSL) is located at the junction of two provinces and Shanghai city. It is

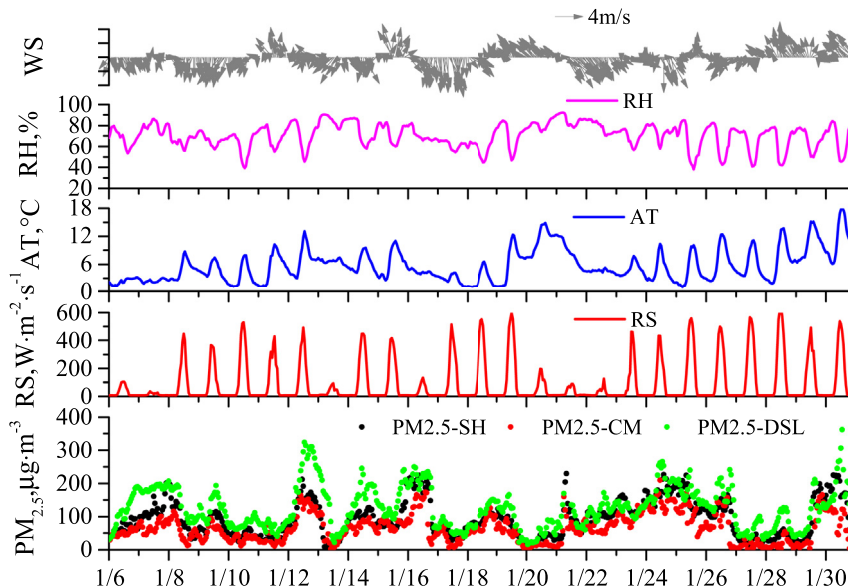


Fig. 6. Time series of the hourly averaged meteorological parameters and PM_{2.5} concentrations at SAES, CM and DSL, YRD.

influenced by all the three areas and the long-range transport outside the modeling domain. As shown from the figure, the monthly average PM_{2.5} at the DSL are contributed by Shanghai (24%), Jiangsu (22%) and Zhejiang (6%), long-range transport constitutes around 48% of the monthly average PM_{2.5} in January 2013. Chongming (CM) is located at the pollution transport channel between Shanghai and Jiangsu. The modeling results indicate that Shanghai constitutes 33% of the monthly PM_{2.5}, Jiangsu contributes 10% and Zhejiang accounts for 2% (Fig. 7).

4.3.2. Temporal change of the PM_{2.5} regional contribution

4.3.2.1. Urban Shanghai. Fig. 8 shows the time series of the regional contribution to hourly PM_{2.5} concentration at urban Shanghai (SAES) during the heavy haze pollution episode in January, 2013. As shown in the figure, the contributions to PM_{2.5} from local and regional are directly related to the hourly weather conditions. Contribution from Zhejiang province increases under the condition of southwest airflow, while contribution from Jiangsu province increases under the northwest wind direction.

During Jan. 6–31 2013, local pollution accumulation is the major contributor to high PM_{2.5} in urban Shanghai area. The average concentration of PM_{2.5} from local accumulation was 55.1 ± 49.8 µg/m³, accounting for 55.4 ± 22.3% to PM_{2.5} in urban Shanghai area.

The predicted maximum hourly concentration of PM_{2.5} from local accumulation was 336.6 µg/m³, accounting for 92.7% of the total high PM_{2.5}.

Super-regional transport outside the D04 modeling domain is the second largest regional contributor to PM_{2.5} in urban Shanghai area, causing the average PM_{2.5} concentration of 36.5 ± 29.2 µg/m³, accounting for 38.4 ± 20.0% of the average PM_{2.5}. The pollution sources from south Jiangsu also have a certain impact on PM_{2.5} in Shanghai, with the contribution of 4.4 ± 7.1%.

However, the regional contribution to PM_{2.5} in Shanghai also has remarkable difference within the month under the influence of meteorological conditions. During Jan. 29–30, local source contributed a majority of the high PM_{2.5} pollution, since the pollution was difficult to diffuse under the unfavorable meteorological conditions of low wind speed. Long-range transport increased the contribution of high pollution during Jan. 13–16, and played a leading role in the continuous high pollution from Jan. 21–24.

The regional contributions to PM_{2.5} in urban Shanghai area from south Jiangsu and north Zhejiang are 4.4% and 1.8%, respectively. The pollution contribution from south Jiangsu area is three times that of north Zhejiang, because the dominant wind direction in winter in China is northwest. However, the contribution from north

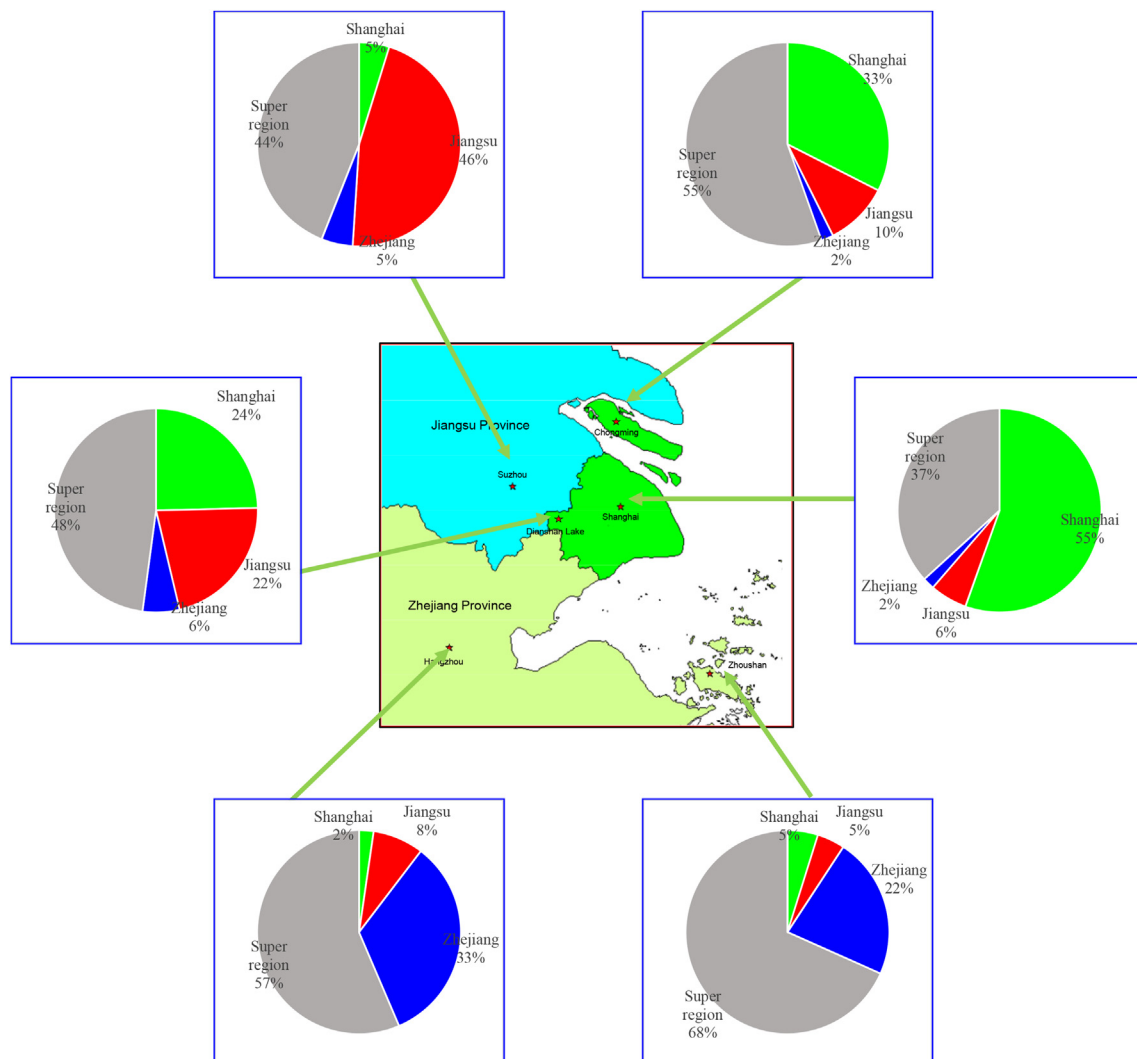


Fig. 7. Regional contribution to PM_{2.5} in the YRD in January, 2013.

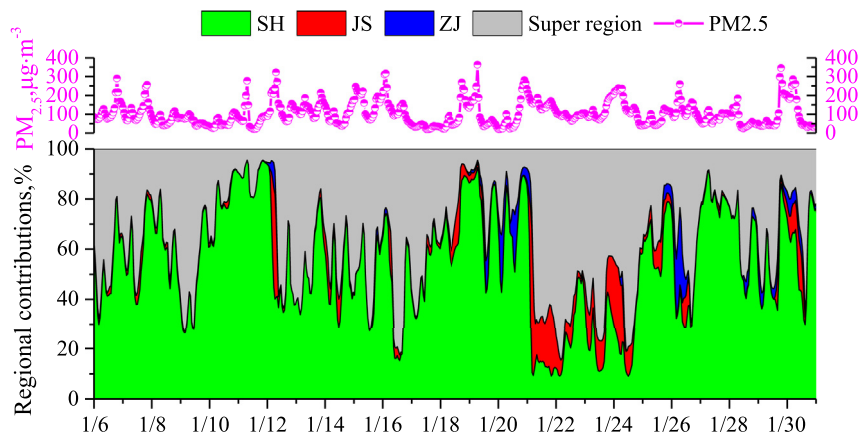


Fig. 8. Time series of the region contributions to PM_{2.5} in urban Shanghai.

Jiangsu is calculated in the influence of long-range transport, thus, the contribution from Jiangsu region is higher than the current result.

4.3.2.2. Urban Suzhou. Fig. 9 shows the time series of the regional contribution to hourly PM_{2.5} concentrations in Suzhou during the haze pollution episode in January, 2013. During Jan. 6–31, local pollution accumulation in Jiangsu province is the major contributor to high PM_{2.5} in urban Suzhou area. The average concentration of PM_{2.5} from local accumulation was $50.2 \pm 35.9 \mu\text{g}/\text{m}^3$, accounting for $46.0 \pm 17.9\%$ to PM_{2.5} in urban Suzhou area. The maximum hourly concentration of PM_{2.5} from local accumulation was $215.1 \mu\text{g}/\text{m}^3$, accounting for 92.8% of the total high PM_{2.5}.

Long-range transport outside the D04 modeling domain is the second largest regional contributor to PM_{2.5} in Suzhou, causing the average PM_{2.5} concentration of $47.9 \pm 32.5 \mu\text{g}/\text{m}^3$, accounting for $38.4 \pm 20.0\%$ of the average PM_{2.5}. The pollution sources from south Zhejiang and Shanghai also have a certain impact on PM_{2.5} in Suzhou, with the contribution of $5.4 \pm 9.6\%$ and $4.5 \pm 10.3\%$, respectively.

4.3.2.3. Urban Hangzhou. Fig. 10 shows the time series of the regional contribution to hourly PM_{2.5} concentrations in Hangzhou during the same haze pollution episode. As the location of the receptor in Hangzhou is close to the southwest boundary of the modeling domain, it is predicted that the super-regional transport is the largest contributor to its PM_{2.5}, accounting for $58.6 \pm 23.1\%$.

Local pollution accumulation in Zhejiang province is the second largest contributor to high PM_{2.5} in urban Hangzhou area. The average concentration of PM_{2.5} from local accumulation was $34.8 \pm 27.4 \mu\text{g}/\text{m}^3$, accounting for $32.2 \pm 18.3\%$ to PM_{2.5} in urban Suzhou area.

4.3.2.4. Zhoushan. As Zhoushan is located in the southeast of Zhejiang province, and there is relatively small anthropogenic emissions around, it is predicted that its PM_{2.5} is mainly coming from long-range transport, with the average contribution of $68.8 \pm 17.5\%$. Zhejiang province constitutes $26.5 \pm 18.3\%$. The lower local contribution is in contrast to Shanghai, Hangzhou and Suzhou (Fig. 11).

4.3.2.5. ChongMing. Chongming is located in the transport path between Shanghai and Jiangsu, therefore, both the two regions impose influence on its high PM_{2.5}. The modeling results indicate that Shanghai contributes $34.2 \pm 24.1\%$. Jiangsu province constitutes $8.0 \pm 9.4\%$, while super-regional transport accounts for $33.8 \pm 36.0\%$ (Fig. 12).

4.3.2.6. Dianshan Lake. As a joint location among the two provinces and Shanghai city, the high PM_{2.5} at Dishan Lake is influenced by Shanghai ($24.8 \pm 23.8\%$), Jiangsu ($20.8 \pm 16.6\%$), Zhejiang ($6.0 \pm 11.1\%$) and super-regional transport ($48.4 \pm 21.4\%$) together. Under different meteorological conditions, the contribution ratio differs quite a lot (Fig. 13)

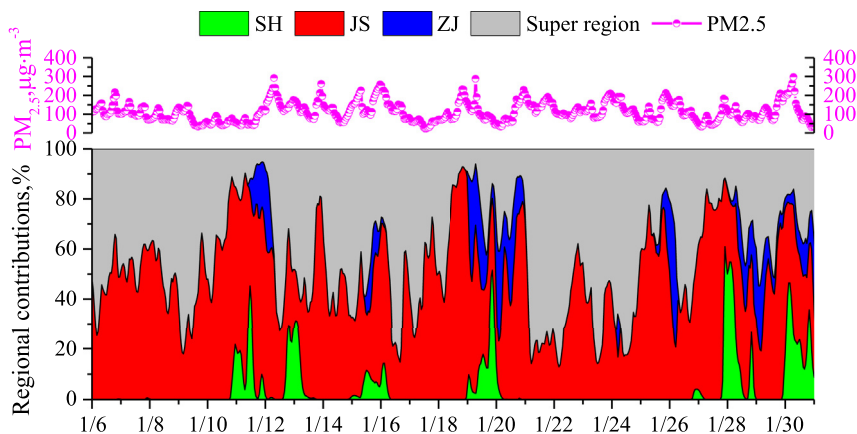


Fig. 9. Time series of the region contributions to PM_{2.5} in Suzhou.

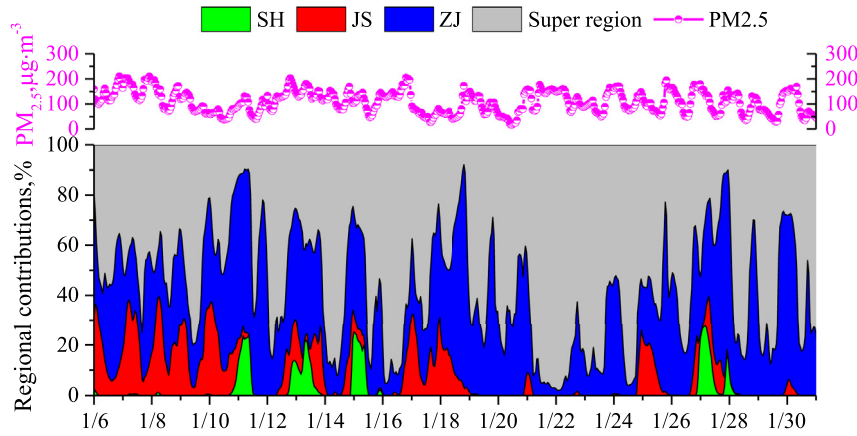


Fig. 10. Time series of the region contributions to PM_{2.5} in Hangzhou.

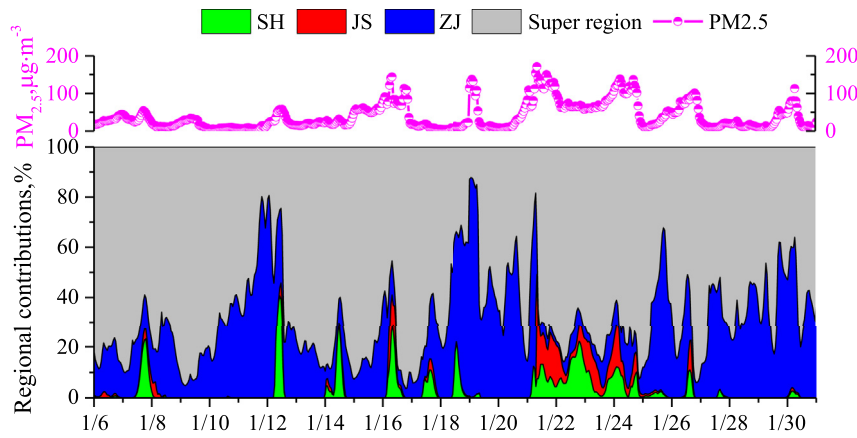


Fig. 11. Time series of the regional contributions to PM_{2.5} in Zhoushan.

4.3.3. Regional emission source contribution

The model predicted source category contribution to PM_{2.5} at the six receptors in the YRD are shown in Fig. 14. As shown in the figure, the high PM_{2.5} concentration was mainly due to precursor emissions from combustion (including coal combustion, oil and gas consumption), industrial processing (including steel making, coking, cement production, petrochemical and chemical processes, etc), mobile source (including vehicle exhaust, ships, and off-road emissions) and fugitive dust.

Among all the receptors, combustion is a prominent source category to PM_{2.5}, with the average contribution ranging between 21.7 and 37.3%. Statistical data shows that the total energy consumption in the Yangtze River Delta in 2012 was 0.58 billion tons of coal equivalent, the coal consumption was 0.48 billion tons, the oil consumption was 78.91 million tones, and the natural gas was 22.4 billion cubic meters (NBS, 2013a,b). This huge energy consumption amount causes a heavy burden to the serious air pollution in the YRD region.

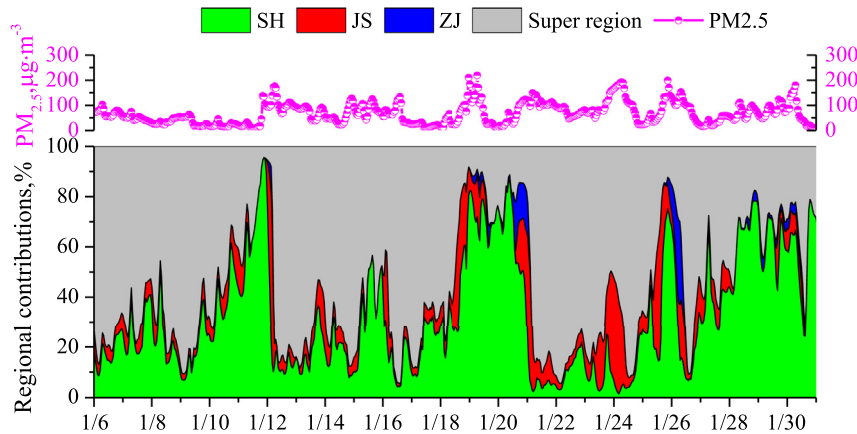


Fig. 12. Time series of the regional contributions to PM_{2.5} in Chongming.

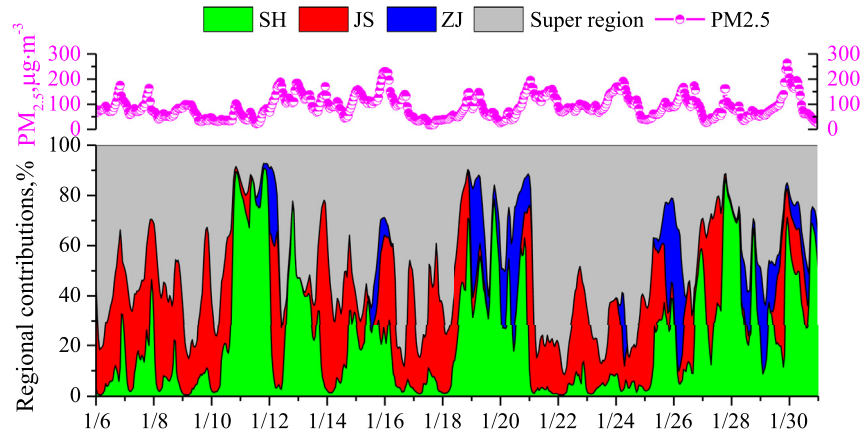


Fig. 13. Time series of the regional contributions to PM_{2.5} in Dianshan Lake.

The contribution from industrial processing ranges between 12.7 and 38.7%. This is mainly because the industry is still heavy in the YRD region. In 2012, the production amount of steel, cement,

and ethylene reached 0.17 billion, 0.29 billion and 4.38 million tons, respectively (NBSC, 2013a). During the industrial processing, lots of fine particles were emitted. In addition, since there are many

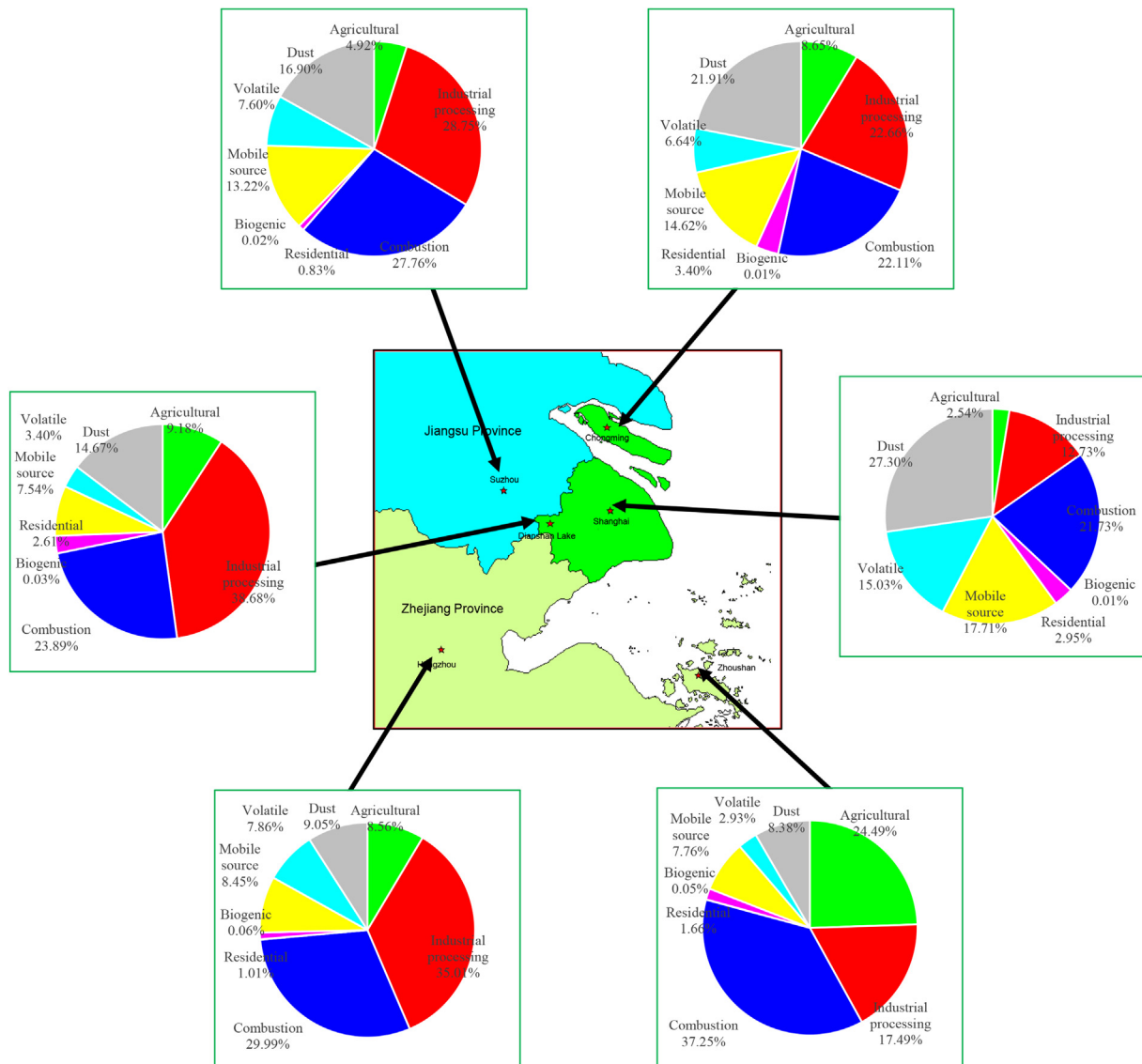


Fig. 14. Source category contribution to PM_{2.5} in the YRD in January, 2013.

photochemical enterprises in the region, lots of volatile organic compounds are emissions during industrial processing, producing gas precursors of secondary organic aerosol (SOA).

Contributions to $PM_{2.5}$ from mobile emissions range between 7.5 and 17.7% in this episode, which is also very significant. Statistical data shows that the total vehicle stock in the YRD region in 2012 was 17.78 million (NBSC, 2013b). In urban area, its contribution is much higher than the rural area (Dianshan Lake, Zhoushan).

Dust is also significant, causing a percentage between 8.4 and 27.3% at different locations.

In rural areas like Zhoushan and Dishan Lake, the contributions to $PM_{2.5}$ from agriculture is very important since there are lots of ammonia emissions from livestock and poultry breeding, and fertilizer application.

4.3.4. Temporal change of the $PM_{2.5}$ source contribution

4.3.4.1. Urban Shanghai. Fig. 15 shows the time series of the source contributions to $PM_{2.5}$ in Shanghai from nine major emission sectors within the D04 simulation area of the Yangtze River Delta during the heavy pollution episode in January, 2013. As shown in the figure, various dust sources within the modeling domain contributes obviously to primary $PM_{2.5}$, with the hourly concentration contribution of $17.3 \pm 15.3 \mu\text{g}/\text{m}^3$, accounting for $28.3 \pm 8.9\%$ of the total $PM_{2.5}$. Primary fine particulate matter and the volatile organic compounds (VOCs) emitted from industrial processing contribute significantly to $PM_{2.5}$ in Shanghai during the whole pollution episode, with the average $PM_{2.5}$ concentration contribution of $8.1 \pm 9.2 \mu\text{g}/\text{m}^3$, accounting for $13.2 \pm 9.0\%$ of the total $PM_{2.5}$. The precursors, NO_x , SO_2 , and primary fine particles from industrial combustion like industrial boilers, kilns and power plants are the main sources of high $PM_{2.5}$ concentration, with the contribution of $13.7 \pm 17.4 \mu\text{g}/\text{m}^3$ ($19.6 \pm 8.7\%$). From this result, the most obvious pollution source is industry, including precursors from fossil fuel combustion and industrial process emissions, accounting for more than 30% of the total $PM_{2.5}$. The mobile source, including vehicles and ships, also contribute to $PM_{2.5}$, with the average concentration of $11.2 \pm 11.1 \mu\text{g}/\text{m}^3$ ($17.0 \pm 5.6\%$), due to the huge NO_x emission amount. Volatile source mainly include VOCs emissions from cooking fume, oil-gas evaporation and paintings, which is a significant precursor of secondary organic aerosol (SOA) (Emanuelsson et al., 2014; Inomata et al., 2014; Li et al., 2015), with the average contribution of $9.5 \pm 8.7 \mu\text{g}/\text{m}^3$ ($15.9 \pm 7.7\%$).

4.3.4.2. Urban Suzhou. Fig. 15 shows the time series of the source contributions to $PM_{2.5}$ in urban Suzhou from major emission sectors within the D04 simulation area of the Yangtze River Delta during the heavy pollution episode in January, 2013. As shown in the figure, combustion is the largest contributor to ambient $PM_{2.5}$, with the hourly concentration contribution of $16.9 \pm 13.4 \mu\text{g}/\text{m}^3$, accounting for $28.4 \pm 9.2\%$ of the total $PM_{2.5}$. Industrial processing also contribute significantly to $PM_{2.5}$ in Suzhou during the whole pollution episode, with the average $PM_{2.5}$ concentration contribution of $17.5 \pm 16.4 \mu\text{g}/\text{m}^3$, accounting for $27.5 \pm 10.5\%$ of the total $PM_{2.5}$. The mobile source, including vehicles and ships, also contribute to $PM_{2.5}$, with the average concentration of $8.1 \pm 6.9 \mu\text{g}/\text{m}^3$ ($13.0 \pm 4.6\%$), due to the huge NO_x emission amount.

4.3.4.3. Urban Hangzhou. Fig. 16 shows the time series of the source contributions to $PM_{2.5}$ in Hangzhou from eight major emission sectors within the D04 simulation area of the Yangtze River Delta during the heavy pollution episode in January, 2013. As shown in the figure, industrial process contributes most to $PM_{2.5}$ in Hangzhou, with the hourly concentration contribution of $16.0 \pm 14.3 \mu\text{g}/\text{m}^3$, accounting for $34.4 \pm 11.3\%$ of the total $PM_{2.5}$. Combustion is the second largest contributor, with the hourly concentration contribution of $13.7 \pm 12.7 \mu\text{g}/\text{m}^3$, accounting for $25.6 \pm 9.6\%$ of the total $PM_{2.5}$. Mobile source contributes $8.8 \pm 3.3\%$ of the total $PM_{2.5}$, which changes with meteorological conditions.

4.3.4.4. Zhoushan. Fig. 17 shows the time series of the source contributions to $PM_{2.5}$ in Zhoushan from eight major emission sectors within the D04 simulation area of the Yangtze River Delta during the heavy pollution episode in January, 2013. As shown in the figure, combustion is also the most important contributor to $PM_{2.5}$, accounting for $27.5 \pm 13.0 \mu\text{g}/\text{m}^3$. Compared to other receptors, the contribution from agriculture is very prominent, with the ratio of $31.7 \pm 13.9\%$. This is mainly because the ammonia emissions from agricultural sector in Zhoushan is the major source, which is a precursor of NH_4^+ in the $PM_{2.5}$ components. Mobile source contributes $7.1 \pm 3.9\%$, which is also not negligible in Zhoushan (Fig. 18).

4.3.4.5. ChongMing. For the air pollution transport path in Chongming, the major source categories contributing to $PM_{2.5}$ include industrial process ($21.3 \pm 9.4\%$), fugitive dust ($22.9 \pm 7.9\%$),

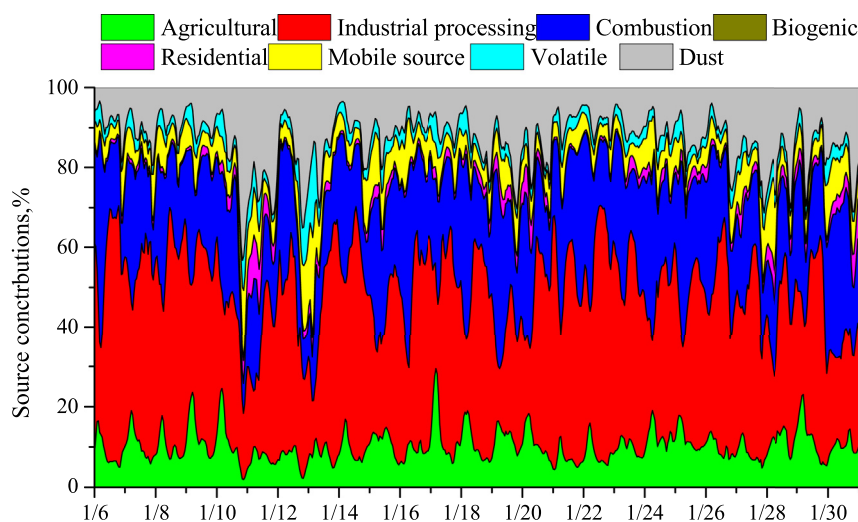


Fig. 15. Source contributions to hourly $PM_{2.5}$ in urban Shanghai from the YRD modeling domain.

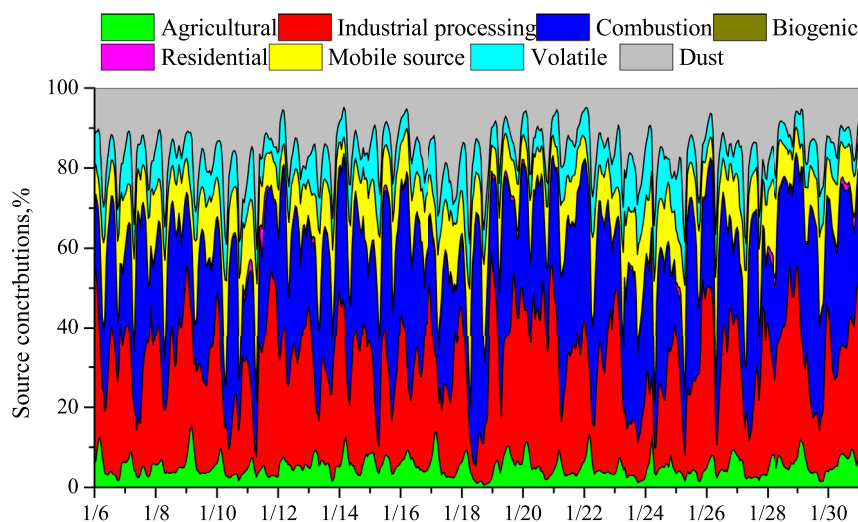


Fig. 16. Source contributions to hourly $PM_{2.5}$ in Suzhou from the YRD modeling domain.

mobile source ($14.5 \pm 4.9\%$), agriculture ($13.9 \pm 9.6\%$), combustion ($14.6 \pm 11.2\%$) and residential ($5.3 \pm 4.4\%$) (Fig. 19).

4.3.4.6. *Dianshan Lake*. Dianshan Lake is influenced by almost all the emission categories due to its location. The major source categories contributing to $PM_{2.5}$ at Dianshan Lake include industrial process ($39.2 \pm 12.3\%$), combustion ($23.8 \pm 8.0\%$), fugitive dust ($13.6 \pm 7.1\%$), agriculture ($10.4 \pm 4.0\%$), mobile source ($6.7 \pm 3.3\%$), and residential ($2.8 \pm 2.6\%$) (Fig. 20).

4.4. Source apportionment of the major chemical components in $PM_{2.5}$ in the YRD

Table 4 shows the statistical analysis of the contribution of local anthropogenic sources to major chemical components of $PM_{2.5}$ during the pollution episode in eastern China in January, 2013. As shown in the table, emissions from the fuel combustion in industrial boilers, furnaces and coal-burned power plants within the YRD region are the main contributors to sulfate and nitrate, ranging between 37.3–72.7% and 45.0–73.8% at different receptors, respectively. Ammonium salt is mostly coming from agricultural

source, including livestock and poultry breeding, fertilizer application, and ammonia volatile emissions from urban anthropogenic sources, accounting for 18.9%–92.5% and 4.8%–66.3%, respectively. Organic carbon mainly comes from mobile source and volatile source. Mobile source contributes a majority of elemental carbon, the contribution percentage ranges between 21.8 and 73.1% at different receptors. In urban Shanghai area, the contributions from combustion source to SO_4^{2-} , NO_3^- , NH_4^+ , OC and EC are 51.4%, 53.5%, 0.8%, 10.7% and 1.6%, respectively. Mobile source has obvious contribution to each component, the contribution percentages to SO_4^{2-} , NO_3^- , NH_4^+ , OC and EC are 17.8%, 34.0%, 10.6%, 29.7% and 73.1%, respectively. It's meaningful to reduce $PM_{2.5}$ and its major chemical components by controlling combustion source and mobile source in urban areas in the YRD region.

5. Conclusions

A heavy winter air pollution episode occurred in eastern China in January, 2013, which is selected to do a source apportionment case study in the YRD region. The CAMx three dimensional model with particulate matter source apportionment technology (PSAT) is

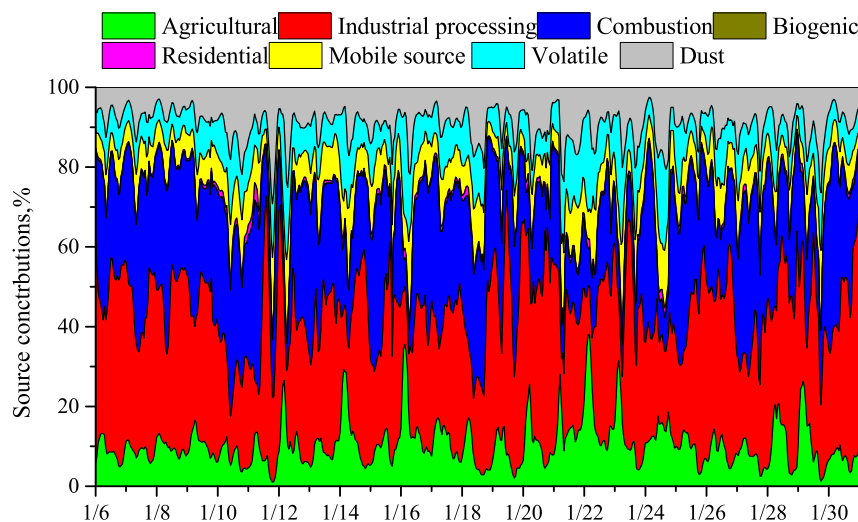


Fig. 17. Source contributions to hourly $PM_{2.5}$ in Hangzhou from the YRD modeling domain.

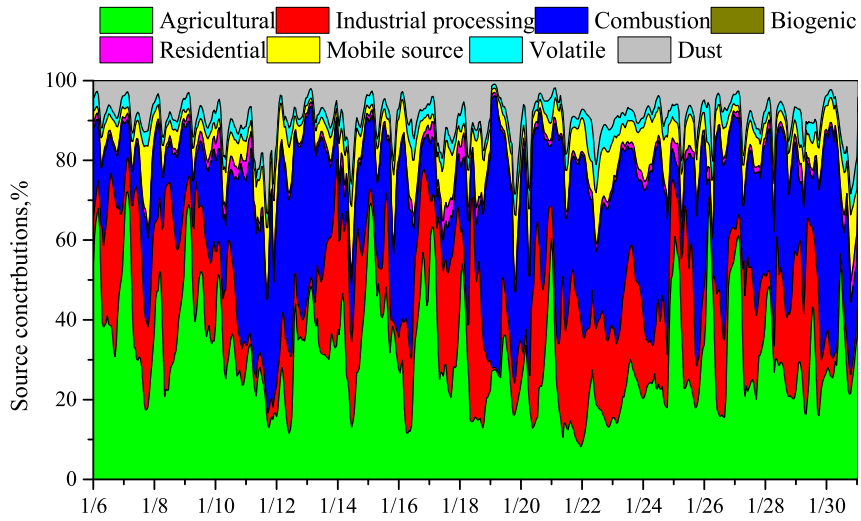


Fig. 18. Source contributions to hourly $PM_{2.5}$ in Zhoushan from the YRD modeling domain.

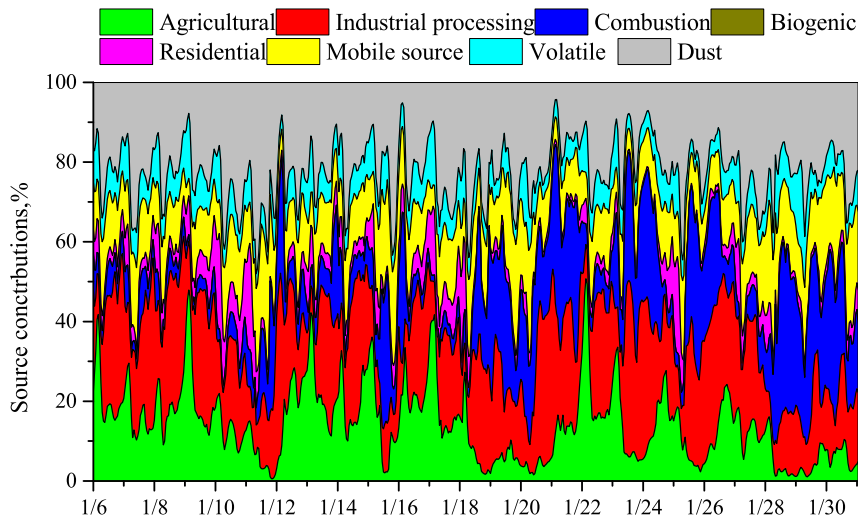


Fig. 19. Source contributions to hourly $PM_{2.5}$ in Chongming from the YRD modeling domain.

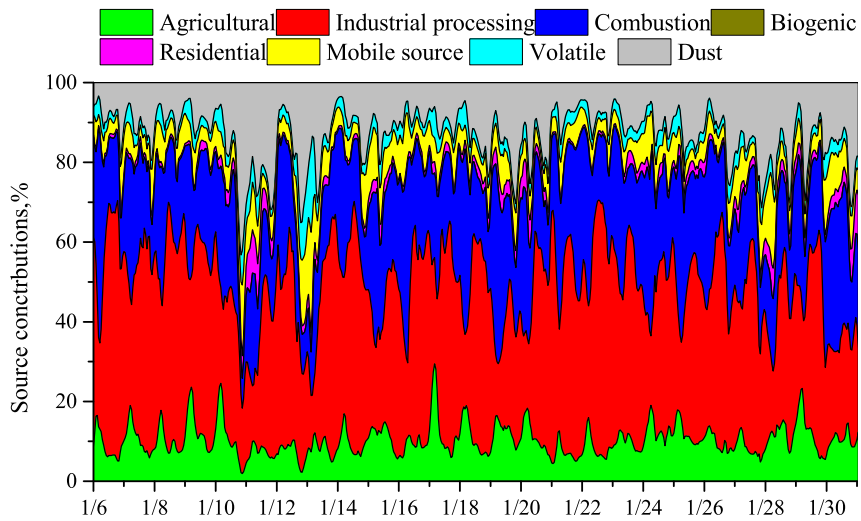


Fig. 20. Source contributions to hourly $PM_{2.5}$ in Dianshan Lake from the YRD modeling domain.

Table 4
Source contributions to the major chemical compositions of PM_{2.5} in major cities of the YRD.

	Shanghai					Suzhou					Hangzhou				
	SO ₄ ²⁻	NO ₃ ⁻	NH ₄ ⁺	OC	EC	SO ₄ ²⁻	NO ₃ ⁻	NH ₄ ⁺	OC	EC	SO ₄ ²⁻	NO ₃ ⁻	NH ₄ ⁺	OC	EC
Combustion	51.4%	53.5%	0.8%	10.7%	1.6%	63.3%	73.8%	0.7%	4.0%	3.9%	57.3%	69.0%	3.2%	5.0%	5.2%
Agriculture	0.0%	0.1%	18.9%	0.4%	0.1%	0.0%	0.1%	35.3%	0.0%	0.0%	0.0%	0.1%	50.3%	0.0%	0.0%
Industrial processing	22.7%	2.2%	3.0%	9.2%	9.4%	27.4%	3.3%	12.8%	53.7%	52.9%	34.6%	7.8%	9.1%	49.6%	50.8%
Biogenic	0.0%	0.0%	0.0%	0.1%	0.0%	0.0%	0.0%	0.0%	0.0%	0.0%	0.0%	0.0%	0.0%	0.0%	0.0%
Residential	2.7%	1.6%	0.5%	4.4%	5.3%	0.8%	0.6%	0.2%	0.0%	0.0%	1.2%	0.9%	0.1%	0.0%	0.0%
Mobile	17.8%	34.0%	10.6%	29.7%	73.1%	6.7%	19.6%	17.3%	25.1%	23.4%	4.6%	20.3%	9.4%	20.1%	21.8%
Volatile	5.1%	8.5%	66.3%	33.0%	2.3%	1.6%	2.6%	33.7%	17.1%	19.8%	2.2%	1.9%	27.9%	25.3%	22.2%
Dust	0.3%	0.0%	0.0%	12.6%	8.2%	0.1%	0.0%	0.0%	0.0%	0.0%	0.1%	0.0%	0.0%	0.0%	0.0%

	Chongming					Dianshan Lake					Zhoushan				
	SO ₄ ²⁻	NO ₃ ⁻	NH ₄ ⁺	OC	EC	SO ₄ ²⁻	NO ₃ ⁻	NH ₄ ⁺	OC	EC	SO ₄ ²⁻	NO ₃ ⁻	NH ₄ ⁺	OC	EC
Combustion	37.25%	45.02%	0.83%	10.28%	1.39%	47.44%	72.39%	0.92%	17.53%	3.48%	72.70%	58.12%	0.20%	19.04%	3.58%
Agriculture	0.04%	0.46%	61.50%	1.75%	0.39%	0.02%	0.13%	64.96%	2.49%	0.74%	0.03%	0.21%	92.48%	4.55%	1.48%
Industrial processing	43.72%	11.33%	3.07%	18.53%	12.25%	47.56%	3.37%	15.11%	33.83%	40.86%	20.57%	9.30%	1.05%	19.63%	15.02%
Biogenic	0.00%	0.00%	0.00%	0.09%	0.00%	0.00%	0.00%	0.00%	0.33%	0.00%	0.00%	0.00%	0.00%	0.73%	0.00%
Residential	4.40%	2.26%	0.15%	15.96%	17.14%	1.53%	0.77%	0.05%	11.49%	15.43%	1.28%	1.45%	0.01%	10.40%	16.51%
Mobile	12.43%	38.53%	7.94%	26.17%	61.35%	2.79%	22.72%	4.87%	13.99%	31.70%	4.42%	28.11%	1.42%	20.09%	55.50%
Volatile	1.94%	2.41%	26.51%	15.47%	0.90%	0.57%	0.63%	14.09%	10.85%	0.82%	0.91%	2.81%	4.83%	17.74%	1.51%
Dust	0.22%	0.00%	0.00%	11.74%	6.59%	0.10%	0.00%	0.00%	9.48%	6.97%	0.09%	0.00%	0.00%	7.82%	6.41%

applied to reveal the contributions from 4 source regions including Shanghai, South Jiangsu, North Zhejiang and super region; 8 source categories including combustion, industrial processing, mobile source, residential, volatile source, dust, agriculture and biogenic emissions to the ambient PM_{2.5} and its 5 major chemical components including SO₄²⁻, NO₃⁻, NH₄⁺, EC, and OC.

During the heavy pollution period from 6th–31st, January, 2013, the hourly PM_{2.5} concentration exceeded 300 µg/m³, among which the local anthropogenic pollution accumulation was the largest contributor to PM_{2.5}, and the second highest contributor is the super-regional transport. Results show that at the 6 different receptors in the YRD region, local accumulation contributions to ambient PM_{2.5} range from 8.6 µg/m³ (Zhoushan) to 55.1 µg/m³ (urban Shanghai), and the contribution percentage range between 22.4% (Zhoushan) and 55.4% (urban Shanghai). Regional contributions to ambient PM_{2.5} range from 12.1 µg/m³ (Zhoushan) to 62.9 µg/m³ (urban Shanghai), accounting for 31.7% (Zhoushan) to 63.2% (urban Shanghai). Super regional contributions to PM_{2.5} at the 6 receptors range from 26.06 µg/m³ (Zhoushan) to 59.1 µg/m³ (Dianshan Lake), accounting for 36.8% (urban Shanghai) to 68.3% (Zhoushan). This result is different from the Pearl River Delta region. Based on Wu's research (Wu et al., 2013), super-regional transport is the major fine particle source, contributing 62% of the total PM_{2.5} in December. This difference is mainly due to the different meteorological conditions and relatively low regional and local anthropogenic emissions in PRD region.

Among the regional contribution part, we mainly consider 8 source categories. Relatively large source category contributions to the airborne PM_{2.5} within the YRD region include combustion, industrial processing, mobile source, dust, and volatile emissions. Fossil fuel combustion contributions to ambient PM_{2.5} from power plants, industrial boilers and kilns range from 4.5 µg/m³ (Zhoushan) to 16.9 µg/m³ (Suzhou), and the contribution percentage range between 21.7% (Urban Shanghai) and 37.2% (Zhoushan). Industrial processing contributions to ambient PM_{2.5} range from 2.1 µg/m³ (Zhoushan) to 17.5 µg/m³ (Hangzhou), and the contribution percentage range between 12.7% (Urban Shanghai) and 38.7% (Dishan Lake). Mobile source emission contributions range from 0.94 µg/m³ (Zhoushan) to 11.19 µg/m³ (urban Shanghai), and the contribution percentage range between 7.5% (Dianshan Lake) and 17.7% (urban Shanghai). Dust also has a certain contribution in the YRD region, accounting for 8.4–27.3% at different receptors. In comparison,

mobile vehicles and marine are the two major fine particle source in the PRD region, contributing 21% (12.2 µg/m³) and 18% (4.7 µg/m³) of the total PM_{2.5} in December (Wu et al., 2013). This is mainly due to the different economic structure and the emission characteristic between the two regions.

As for the source category contribution to PM_{2.5} chemical components in the YRD region, it is found that combustion source contributes the most to sulfate, accounting for 37.3%–72.7%, while it accounts for 45.0%–73.8% to nitrate. Ammonia mainly comes from volatile source and agriculture. Elemental carbon comes from mobile source and industrial processing. The major organic carbon contributors are volatile source and transportation, accounting for 10.8%–33.2% and 14.0%–29.7% respectively at different receptors.

The control of industrial source, power plants, mobile source, dust and volatile source near the surface ground of the Yangtze River Delta region during heavy haze pollution process is very important. As the prominent status of air pollution transport, regional joint prevention and control of air pollution will help to significantly reduce fine particles.

Acknowledgments

This study was supported by the “Chinese National Key Technology R&D Program” via grant No. 2014BAC22B03, the “Chinese National Non-profit Scientific Research Program” via grant No. 201409008, the National Natural Science Foundation of China (NSFC) via grant No. 41205122, and the Key research project from the Science and Technology Commission of Shanghai Municipality Fund Project via grant No. 14DZ1202905. We thank Shanghai Environmental Monitoring Center for providing the observational data to do model verification. We also appreciate the suggestions made by the two anonymous reviewers that helped greatly to improve this paper.

References

- Appel, K.W., Bhawe, P.V., Gilliland, A.B., Sarwar, G., Roselle, S.J., 2008. Evaluation of the community multiscale air quality (CMAQ) model version 4.5: sensitivities impacting model performance; part II particulate matter. *Atmos. Environ.* 42, 6057–6066. <http://dx.doi.org/10.1016/j.atmosenv.2008.03.036>.
- Basart, S., Pay, M.T., Jorba, O., Perez, C., Jimenez-Guerrero, P., Schulz, M., Baldasano, J.M., 2012. Aerosols in the CALOPE air quality modelling system: evaluation and analysis of PM levels, optical depths and chemical composition

- over Europe. *Atmos. Chem. Phys.* 12, 3363–3392.
- Bao, Z., Feng, Y.C., Jiao, L., Hong, S.M., Liu, W.G., 2010. Characterization and source apportionment of PM_{2.5} and PM₁₀ in Hangzhou. *Environ. Monit. China* 26 (2), 44–48.
- Chen, X.L., Feng, Y.R., Li, J.N., Lin, W.S., Fan, S.J., Wang, A.Y., Fong, S.K., Lin, H., Chen, X.L., 2009. Numerical simulations on the effect of sea-land breezes on atmospheric haze over the Pearl River Delta Region. *Environ. Model. Assess.* 14, 351–363.
- Craig, L., Brook, J.R., Chiotti, Q., Croes, B., Gower, S., 2008. Air pollution and public health: a guidance document for risk managers. *J. Toxicol. Environ. Health – Part A Curr. Issues* 71, 588–698.
- Dai, S.G., Zhu, T., Bai, Z.P., 1995. Application and development of receptor models for the source apportionment of airborne particulate matter. *China Environ. Sci.* 15 (4), 252–257.
- Du, H.H., Kong, L.D., Cheng, T.T., Chen, J.M., Du, J.F., Li, L., Xia, X.G., Leng, C.P., Huang, G.H., 2011. Insights into summertime haze pollution events over Shanghai based on online water-soluble ionic composition of aerosols. *Atmos. Environ.* 45, 5131–5137.
- Dunker, A.M., 1981. Efficient calculation of sensitivity coefficients for complex atmospheric models. *Atmos. Environ.* 15, 1155–1161.
- Dunker, A.M., Yarwood, G., Ortmann, J.P., Wilson, G.M., 2002. Comparison of source apportionment and source sensitivity of ozone in a three-dimensional air quality model. *Environ. Sci. Technol.* 36, 2953–2964.
- Emanuelsson, E.U., Mentel, T.F., Watne, A.K., Spindler, C., Bohn, B., Brauers, T., Dorn, H.P., Hallquist, A.M., Häseler, R., Scharr, A.K., Müller, K.P., Pleijel, H., Rohrer, F., Rubach, F., Schlosser, E., Tillmann, R., Hallquist, M., 2014. Parameterization of thermal properties of aging secondary organic aerosol produced by photo-oxidation of selected Terpene mixtures. *Environ. Sci. Technol.* 48, 6168–6176.
- ENVIRON, 2011. CAMx User's Guide Comprehensive Air Quality Model with Extensions Version 5.40. International Corporation.
- Foley, K.M., Roselle, S.J., Appel, K.W., Bhawe, P.V., Pleim, J.E., Otte, T.L., Mathur, R., Sarwar, G., Young, J.O., Gilliam, R.C., Nolte, C.G., Kelly, J.T., Gilliland, A.B., Bash, J.O., 2010. Incremental testing of the community multiscale air quality (CMAQ) modeling system version, 4.7. *Geosci. Model Dev.* 3, 205–226.
- Guo, S., Hu, M., Wang, Z.B., Slanina, J., Zhao, Y.L., 2010. Size-resolved aerosol water-soluble ionic composition in the summer of Beijing: implication of regional secondary formation. *Atmos. Chem. Phys.* 10 (10), 4477–4491.
- Heo, J.B., Hopke, P.K., Yi, S.M., 2009. Source apportionment of fine organic aerosols in Beijing. *Atmos. Chem. Phys.* 9, 8573–8585.
- Huang, C., Chen, C.H., Li, L., 2011. Emission inventory of anthropogenic air pollutants and VOC species in the Yangtze River Delta region, China. *Atmos. Chem. Phys.* 11, 4105–4120.
- Huang, H.J., Liu, H.N., Jiang, W.M., Huang, S.H., Zhang, Y.Y., 2006. Physical and chemical characteristics and source apportionment of PM_{2.5} in Nanjing. *Clim. Environ. Res.* 11 (6), 713–722.
- Huang, K., Zhuang, G., Lin, Y., 2012. Typical types and formation mechanisms of haze in an Eastern Asia megacity, Shanghai. *Atmos. Chem. Phys.* 12, 105–124.
- Huang, W., Tan, J.G., Kan, H.D., Zhao, N., Song, W.M., Song, G.X., Chen, G.H., Jiang, L.L., Jiang, C., Chen, R.J., Chen, B.H., 2009. Visibility, air quality and daily mortality in Shanghai, China. *Sci. Total Environ.* 407, 3295–3300.
- Inomata, S., Sato, K., Hirokawa, J., Sakamoto, Y., Tanimoto, H., Okumura, M., Tohno, S., Imamura, T., 2014. Analysis of secondary organic aerosols from ozonolysis of isoprene by proton transfer reaction mass spectrometry. *Atmos. Environ.* 97, 397–405.
- Kang, H.Q., Zhu, B., Su, J.F., Wang, H.L., Zhang, Q.C., Wang, F., 2013. Analysis of a long-lasting haze episode in Nanjing, China. *Atmos. Res.* 120–121, 78–87.
- Kasibhatla, P., Chameides, W.L., Jonn, J.S., 1997. A three dimensional global model investigation of seasonal variations in the atmospheric burden of anthropogenic sulphate aerosols. *J. Geophys. Res.* 102, 3737–3759.
- Koo, B., Wilson, G.M., Morris, R.E., Dunker, A.M., Yarwood, G., 2009. Comparison of source apportionment and sensitivity analysis in a particular matter air quality model. *Environ. Sci. Technol.* 43, 6669–6675.
- Li, L., Chen, C.H., Fu, J.S., Huang, C., Streets, D.G., Huang, H.Y., Zhang, G.F., Wang, Y.J., Jang, C.J., Wang, H.L., Chen, Y.R., Fu, J.M., 2011. Air quality and emissions in the Yangtze River Delta, China. *Atmos. Chem. Phys.* 11, 1621–1639.
- Li, L., Chen, C.H., Huang, C., Huang, H.Y., Li, Z.P., Fu, J.M., Jang, C.J., Streets, D.G., 2008. Regional air pollution characteristics simulation of O₃ and PM₁₀ over Yangtze River Delta region. *Environ. Sci.* 29 (1), 237–245 (in Chinese).
- Li, J.Y., Cleveland, M., Ziemba, L.D., Griffin, R.J., Barsanti, K.C., Pankow, J.F., Ying, Q., 2015. Modeling regional secondary organic aerosol using the master chemical mechanism. *Atmos. Environ.* 102, 52–61.
- Matthias, V., 2008. The aerosol distribution in Europe derived with the community multiscale air quality (CMAQ) model: comparison to near surface in situ and sunphotometer measurements. *Atmos. Chem. Phys.* 8, 5077–5097.
- Monks, P.S., Granier, C., Fuzzi, S., Stohl, A., Williams, M.L., Akimoto, H., Amann, M., Baklanov, A., Baltensperger, U., Bey, I., Blake, N., Blake, R.S., Carslaw, K., Cooper, O.R., Dentener, F., Fowler, D., Fragkou, E., Frost, G.J., Generoso, S., Ginoux, P., Grewe, V., Guenther, A., Hansson, H.C., Henne, S., Hjorth, J., Hofzumahaus, A., Huntrieser, H., Isaksen, I.S.A., Jenkin, M.E., Kaiser, J., Kanakidou, M., Klimont, Z., Kulmala, M., Laj, P., Lawrence, M.G., Lee, J.D., Liousse, C.M., Maione, McFiggans, G., Metzger, A., Mievville, A., Moussiopoulos, N., Orlando, J.J., O'Dowd, C.D., Palmer, P.I., Parrish, D.D., Petzold, A., Platt, U., Pöschl, U., Prévôt, A.S.H., Reeves, C.E.S., Reimann, Rudich, Y., Sellegri, K., Steinbrecher, R., Simpson, D., ten Brink, H., Theloke, J., van der Werf, G.R., Vautard, R., Vestreng, V., Vlachokostas, Ch., von Glasow, R., 2009. Atmospheric composition change e global and regional air quality. *Atmos. Environ.* 43, 5268–5350.
- NBSC, National Bureau of Statistics, People' Republic of China, 2013a. *China Energy Statistical Yearbook-2012*.
- NBSC, National Bureau of Statistics, People's Republic of China, 2013b. *China Statistical Yearbook-2012*.
- Nenes, A., Pilinis, C., Pandis, S.N., 1998. ISORROPIA: a new thermodynamic model for multiphase multicomponent inorganic aerosols. *Aquat. Geochem.* 4, 123–152.
- Richards, L.W., Alcorn, S.H., McDade, C.C.T., Lowenthal, D., Chow, J.C., Watson, J.G., 1999. Optical properties of the San Joaquin valley aerosol collected during the 1995 integrated monitoring study. *Atmos. Environ.* 33, 4787–4795.
- Schauer, J.J., Cass, G.R., 2000. Source apportionment of wintertime gas-phase and particle-phase air pollutants using organic compounds as tracers. *Environ. Sci. Technol.* 34, 2736–2744.
- Schauer, J.J., Rogge, W.F., Hildemann, L.M., Mazurek, M.A., Cass, G.R., Simoneit, B.R.T., 1996. Source apportionment of airborne particulate matter using organic compounds as tracers. *Atmos. Environ.* 30, 3837–3855.
- Song, Y., Dai, W., Shao, M., Liu, Y., Lu, S.H., Kuster, W., Goldan, P., 2008. Comparison of receptor models for source apportionment of volatile organic compounds in Beijing, China. *Environ. Pollut.* 156, 174–183.
- Subramanian, R., Donahue, N.M., Bernardo-Bricker, A., Rogge, W., Robinson, A.L., 2006. Contribution of motor vehicle emissions to organic carbon and fine particle mass in Pittsburgh Pennsylvania: effects of varying source profiles and seasonal trends in ambient marker concentrations. *Atmos. Environ.* 40, 8002–8019.
- Tie, X.X., Cao, J.J., 2009. Aerosol pollution in China: present and future impact on environment. *Particuology* 7, 426–431.
- U.S.EPA, 2007. Guidance on the Use of Models and Other Analyses for Demonstrating Attainment of Air Quality Goals for Ozone, PM_{2.5} and Regional Haze. Final Rep. EPA-454/B-07–002. USEPA, Research Triangle Park, N. C., 27, p. 711.
- Volkamer, R., Jiménez, J.L., San Martini, F., Dzepina, K., Zhang, Q., Salcedo, D., Molina, L.T., Worsnop, D.R., Molina, M.J., 2006. Secondary organic aerosol formation from anthropogenic air pollution: rapid and higher than expected. *Geophys. Res. Lett.* 33, L17811. <http://dx.doi.org/10.1029/2006GL026899>.
- Wagstrom, K.M., Pandis, S.N., Yarwood, G., Wilson, G.M., Morris, R.E., 2008. Development and application of a computationally efficient particulate matter apportionment algorithm in a three-dimensional chemical transport model. *Atmos. Environ.* 42, 5650–5659.
- Wang, L.T., Wei, Z., Yang, J., Zhang, Y., Zhang, F.F., Su, J., Meng, C.C., Zhang, Q., 2013. The 2013 severe haze over the southern Hebei, China: model evaluation, source apportionment, and policy implication. *Atmos. Chem. Phys. Diss.* 13, 28395–28451.
- Wang, Q., Shao, M., Zhang, Y., Wei, Y., Hu, M., Guo, S., 2009. Source apportionment of fine organic aerosols in Beijing. *Atmos. Chem. Phys.* 9, 8573–8585.
- Wang, Z.F., Li, J., Wang, Z., Yang, W.Y., Tang, X., Ge, B.Z., Yan, P.Z., Zhu, L.L., Chen, X.S., Chen, H.S., Wand, W., Li, J.J., Liu, B., Wang, X.Y., Wand, W., Zhao, Y.L., Lu, N., Su, D.B., 2014. Modeling study of regional severe hazes over Mid-Eastern China in January 2013 and its implications on pollution prevention and control, science China. *Earth Sci.* 57, 3–13. <http://dx.doi.org/10.1007/s11430-013-4793-0>.
- WHO (World Health Organization), 2009. *Global Health Risks: Mortality and Burden of Disease Attributable to Selected Major Risks*, ISBN 978 92 4 156387 1. http://www.who.int/healthinfo/global_burden_disease/GlobalHealthRisks_report_full.pdf.
- Wu, D.W., Jimmy, C.H.F., Yao, T., Alexis, K.H.L., 2013. A study of control policy in the Pearl River Delta region by using the particulate matter source apportionment method. *Atmos. Environ.* 76, 147–161.
- Yarwood, G., Rao, S., Yocke, M., Whitten, G., 2005. Updates to the Carbon Bond Chemical Mechanism: CB05. Final Report prepared for US EPA, Available at: http://www.camx.com/publ/pdfs/CB05_Final_Report_120805.pdf.
- Ying, Q., Kleeman, M.J., 2006. Source contributions to the regional distribution of secondary particulate matter in California. *Atmos. Environ.* 40, 736–752.
- Zhang, Q.H., Zhang, J.P., Xue, H.W., 2010. The challenge of improving visibility in Beijing. *Atmos. Chem. Phys.* 10, 7821–7827.
- Zhang, Q., Streets, D.G., Carmichael, G.R., He, K.B., Huo, H., Kannari, A., Klimont, Z., Park, I.S., Reddy, S., Fu, J.S., Chen, D., Duan, L., Lei, Y., Wang, L.T., Yao, Z.L., 2009. Asian emissions in 2006 for the NASA INTEX-B Mission. *Atmos. Chem. Phys.* 9, 5131–5153.
- Zhang, X.Y., 2007. Aerosol over China and their climate effect. *Adv. Earth Sci.* 22 (1), 12–16.
- Zhang, Y., Vijayaraghavan, K., Seigneur, C., 2005. Evaluation of three probing techniques in a three-dimensional air quality model. *J. Geophys. Res.* 110, D02305. <http://dx.doi.org/10.1029/2004JD005248>.
- Zheng, M., Cass, G.R., Schauer, J.J., Edgerton, E.S., 2002. Source apportionment of PM_{2.5} in the Southeastern United States using solvent-extractable organic compounds as tracers. *Environ. Sci. Technol.* 36, 2361–2371.
- Zhou, M., Chen, C.H., Qiao, L.P., Lou, S.R., Wang, H.L., Huang, H.Y., Wang, Q., Chen, M.H., Chen, Y.R., Li, L., Huang, C., Zou, L.J., Mu, Y.Y., Zhang, G.F., 2013. The chemical characteristics of particulate matters in Shanghai during heavy air pollution episode in Central and Eastern China in January 2013. *Acta Sci. Circumst.* 33 (11), 3118–3126 (in Chinese).